BOR DERGİSİ
JOURNAL OF BORON
https://dergipark.org.tr/boron

A novel boron nitride quantum dots-based fluorescent sensing platform for selective detection of Fe^{3+}

Duygu Kuru [1,*]

[1]*Bilecik Seyh Edebali University, Faculty of Engineering, Department of Chemical Engineering, Bilecik, 11100, Türkiye*

ARTICLE INFO

Article history:
Received September 25, 2024
Accepted January 15, 2025
Available online March 31, 2025

Research Article

DOI: 10.30728/boron.1556075

Keywords:
Boron nitride quantum dots
Fluorescent sensing platform
Metal ion sensing
Nanocomposite film
PMMA

ABSTRACT

In this study, boron nitride quantum dots (BNQDs) and polymethyl methacrylate (PMMA) nanocomposite films were produced to be used as a metal sensing material. BNQDs were synthesized from boric acid and urea using the hydrothermal method. The selectivity of PMMA/BNQDs nanocomposite films as fluorescent sensing platforms was tested for different metal ions (Fe^{3+}, Na^{+} Zn^{2+}, Mg^{2+}, and Ca^{2+}). The morphological, structural, and chemical properties of the produced films were determined by scanning electron microscope (SEM), high-resolution transmission electron microscopy (HRTEM), Fourier transform infrared (FT-IR) spectroscopy, and atomic force microscopy (AFM) analyses. The optical properties of the films were determined by ultraviolet-visible spectrophotometer (UV-Vis). Fluorescence and sensing properties were determined using photoluminescence (PL) spectroscopy analysis. SEM and transmission electron microscopy (TEM) analyses confirmed the strong bonding and homogeneous distribution between the BNQDs and the PMMA. FT-IR and TEM analyses proved the formation of BNQDs. PMMA-BNQDs nanocomposite film showed selective fluorescence quenching properties for Fe^{3+} ions. The fluorescence intensity of the nanocomposite films showed a good linear relationship between 0-60 µM for Fe^{3+}. In addition, it showed good sensitivity to detect Fe^{3+} ions in drinking water. Thus, this fluorescent sensing platform can be selective and sensitive in the 0-60 µM concentration range with a limit of detection (LOD) of 4.06 µM.

1. Introduction

The growth in the industrial area and the rapid increase in the population bring about water pollution [1]. Heavy metal ions in water negatively impact the environment and human health [2]. As it is known, it is impossible to live without water consumption, and for this reason, so much research is carried out to ensure that the water is clean and does not threaten human health. Polluted water can contain a wide variety of ions such as Cu^{2+}, Cd^{2+}, Co^{2+}, Ni^{2+}, Al^{3+}, Pb^{2+}, Hg^{2+}, Fe^{3+}, Fe^{2+}, and these ions can combine to form more dangerous compounds [3]. These highly toxic compounds cannot decompose and, as a result, continue accumulating on the earth, causing harm to the human body [4]. This situation has encouraged researchers to find new materials to remove and sense metal ions.

Quantum dots are used not only in bio-imaging or solar cells but also frequently in chemical sensor applications [5]. Boron nitride quantum dots (BNQDs) are promising sensor materials, especially in detecting fluorescent-based metal ions or gases, due to their photoluminescence emission, good solution dispersion, tunable band gap, and biocompatibility [6]. There are several studies in the literature in which BNQDs are used as metal ion-selective in solution form. However, BNQDs, unlike carbon quantum dots, are still open to development as metal sensors, as they are newly discovered. Huo et al. used BNQDs, which were produced by hydrothermal synthesis methods using boric acid and melamine to detect ferric ions in aqueous solutions. They concluded that prepared quantum dots could be effectively used as a valuable fluorochrome [7]. Liu et al. similarly used BNQDs produced by hydrothermal synthesis to detect different concentrations of Fe^{2+} and Fe^{3+} ions in the aqueous medium. In their study, they also simulated hydrothermal reaction and fluorescence properties using density simulated functional theory (DFT). They concluded that as the concentration of Fe^{2+} and Fe^{3+} increased, the fluorescence intensity of BNQDs was quenched [8]. Peng et al. exfoliated hexagonal boron nitride treated with hydrazine (N_2H_4) in an ethanol-water mixture and then obtained BNQDs by hydrothermal synthesis. The obtained BNQDs-based sensor material shows potential for selectively detecting 2,4,6-trinitrophenol in natural water without

*Corresponding author: duygu.gokdai@bilecik.edu.tr

any pretreatment process [9]. Wang et al. used hexagonal boron nitride quantum dot probes for the detection of Hg^{2+} ions. In the presence of Hg^{2+} ions in the medium, BNQDs created a peak at 560 nm under 280 nm excitation [10]. In the study of Han et al., the fluorescence effects of BNQDs on different metal ions were determined. It was observed that fluorescence peaks of both Fe^{3+} and Cu^{2+} ions could be quenched in the presence of BNQDs [11].

While there are several studies in the literature investigating the fluorescence properties of BNQDs in solution, no study has been found in which BNQDs/polymer nanocomposite films are used as test surfaces for metal ion detection. While metal ions can be detected in an aqueous solution or with the help of probes or devices, the fact that these methods are expensive, and the sensor materials can be prepared as a result of complex processes. This situation has led researchers to find practical and disposable economic methods such as fluorescent test papers or composite films [12-14]. In this method, chemical ions on the surface interact chemically with metals when test papers are immersed in a solution including metal ions. As a result of this interaction, the color change on the test paper can instantly detect metal ions. In their study, Wang et al. showed the sensor activity of the graphene quantum dots by coating them on the surface with the polyvinyl alcohol (PVA) polymer in different metal solutions [15]. Dalal et al. developed a sensor for detecting Fe^{3+} ions doped with polymer-based carbon dots. These sensors based on polyether amine showed high sensitivity in aqueous media with a limit of detection (LOD) value of 162 nm [16]. In 2021, Shirani et al. developed a polymer-integrated silica quantum dot-based sensor with a 1 nm LOD for indoxacarb [17].

Polymethyl methacrylate (PMMA) has a hydrophilic structure with a water contact angle of 68°. PMMA has many advantages over other polymers, such as superior environmental stability and scratch and UV resistance [18]. In addition, there are also studies showing that it is produced as a composite with boron nitride and that boron nitride is effectively distributed in this polymer [19,20]. Wang et al. also used $CsPbBr_3$ perovskite quantum dot/PMMA fiber structures in the detection of Cu^{2+} ions from water in their study [21]. In another study, PMMA films were produced using the electrospun method with fluorescent poly(amidoamine) to detect heavy Co^{2+} ions in water [22].

Some properties of polymers, such as low selectivity and sensitivity and weak photoluminescence properties, may limit their use, especially in heavy metal detection. Low-dimensional quantum dots are very effective in creating metal detection platforms due to their superior optical-electronic and chemical diversity properties. In addition, polymers provide an excellent matrix for the dispersion of these low-dimensional nanoparticles and enable them to use their properties as nanocomposite films [23]. Based on this motivation, in this study, after the BNQDs were formed by the hydrothermal synthesis method, they were incorporated into the PMMA polymer to produce nanocomposite film, and fluorescence properties were determined for different metal ions (Fe^{3+}, Na^{+}, Zn^{2+}, Mg^{2+}, and Ca^{2+}) for the first time. In addition, the effect of different concentrations of Fe^{3+} aqueous solutions (0-100 µM) on the fluorescence properties of nanocomposite films was also investigated. This test surface has been developed as an environmentally friendly, economical, and practical sensor material that detects metal contamination in aqueous solutions.

2. Materials and Methods

2.1. BNQDs and PMMA/BNQDs Fluorescent Sensing Platform Preparation

BNQDs were produced using the hydrothermal synthesis method. Here, the dispersant phase in the BNQD solution is 10 mL of ethanol, 5 mL of distilled water for boric acid, and 10% ammonia solution for urea. Details of the synthesis of BNQDs were given in our previous work [24]. A certain amount of PMMA (Sigma-Aldrich, US) was dissolved to form the composite films in 50 mL acetone. Then, the PMMA solution was added to the BNQDs solution at a weight ratio of 1:0.2. The solution was sonicated for 1 hour and stirred for 6 hours using a magnetic stirrer. The resulting mixture was kept in the beaker and dried completely under ambient conditions, and then it was obtained as BNQDs-doped PMMA composite films. The flow chart of the experimental method is shown in Figure 1.

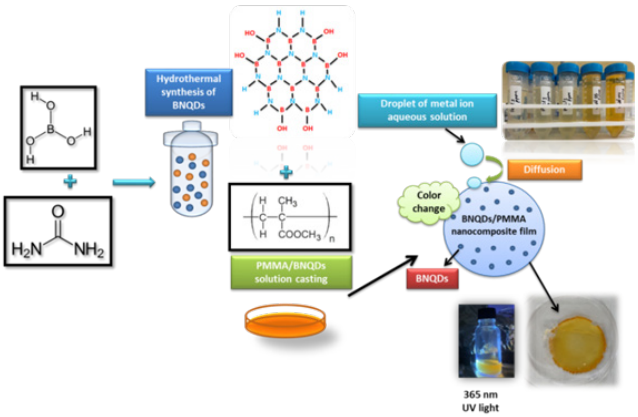

Figure 1. Schematic flow chart of the process

2.2. Metal Ion Detection of PMMA/BNQDs Fluorescent Sensing Platform

Heavy metal solutions were prepared from their salts and nitrates. Fe^{3+} prepared from $FeCl_3$, Na^{+} from NaCl, Zn^{2+} from $Zn(NO_3)_2$, Mg^{2+} from $MgCl_2$ and Ca^{2+} from $CaCl_2$. In a typical process, a certain amount of (100 µM) metal ions (Fe^{3+}, Na^{+}, Zn^{2+}, Mg^{2+}, and Ca^{2+}) were added into water, and then the PMMA/BNQDs films were immersed in the different metal ions aqueous solutions. Different concentrations (0, 20, 45, 60,

80, and 100 μM) of Fe^{3+} aqueous solutions were prepared, and the films were immersed for 3 minutes. PL measurements were carried out after the films were removed from the solution.

2.3. Characterization

The morphological and chemical analysis was performed using SEM (Zeiss Supra 40VP, Germany) at different magnifications (25 and 75 kX for PMMA and 10 and 40 kX for PMMA-BNQDs composite film), high-resolution TEM (HRTEM) (FEI TALOS F200S TEM, 200 kV, US), and FT-IR (Agilent Technologies, Cary 630, between 400-4000 cm^{-1}, US) analysis. Optical properties of the composites were determined by UV-Vis spectrophotometer (Agilent Technologies, Cary 60 UV-Vis, US) and photoluminescence properties were determined by PL spectroscopy (Dongwoo optron, matched with maple II HeCd laser, 532 nm, between 200 and 800 nm, South Korea). AFM analyzed the size of the produced composite with the scan size fixed to 1 μm × 1 μm (Park Systems, South Korea).

3. Results and Discussion

The most priority analyses to define the optical properties of quantum dots are the determination of absorption and fluorescence spectrum. Figure 2a shows the UV-Vis spectrum of pure and composite samples.

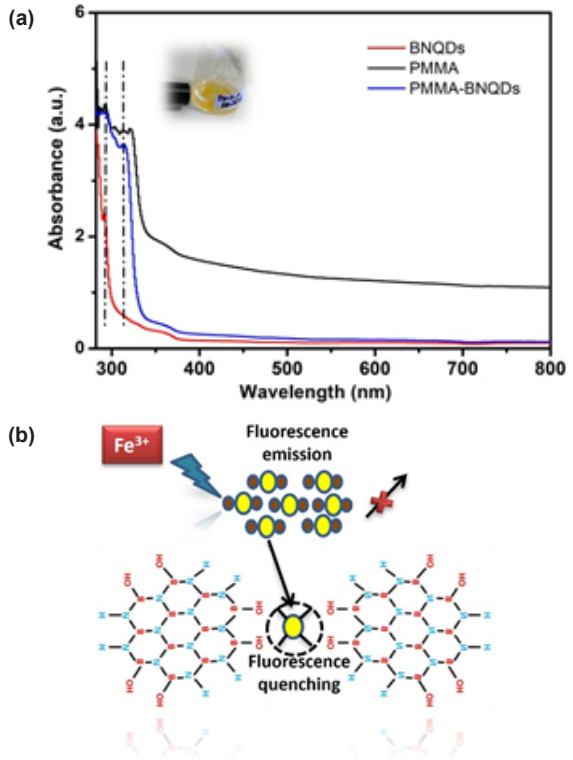

Figure 2. UV-Vis spectrum of the pure and composite samples; inset: PMMA-BNQDs composite solution appears as a blue-green color under 365 nm UV light (a), possible fluorescence quenching mechanism of PMMA/BNQDs film by Fe^{3+} (b)

Two main peaks appear around 280 and 290 nm in the absorption spectrum of the obtained BNQDs. While the intense peak at 280 nm is defined as the peak arising due to band transitions in quantum dots, the weak peak at 290 nm is due to the change in the band gap. The main reason for this band gap change is the functional groups attached to the surface of the quantum dots [25-27]. Two different peaks occur at 280 and 315 nm in the absorption spectrum of the PMMA-BNQDs composite film. These are the peaks from BNQDs and PMMA polymer, respectively. Compared with the absorption spectrum of BNQDs, the peak at 280 nm in the composite sample did not show any shift, indicating that the quantum dots were distributed homogeneously in the PMMA [28]. Figure 2b shows the possible fluorescence capture mechanism of iron ions by the PMMA-BNQDs composite film.

Boron nitride has an electron affinity towards metal ions thanks to the abundance of hydroxyl and amino groups at the corners of the quantum dots. When metal ions form a complex with the surface of BNQDs, the basic level of fluorescence is quenched and turns into a non-fluorescent compound. After photoexcitation, the BNQDs metal ion complex returns to its ground state by absorbing the blocked light and emission [29]. Figure 3a includes the IR spectrum of the produced BNQDs. FT-IR analysis is one of the most effective methods for determining the chemical structure and analysis of functional groups in the sample.

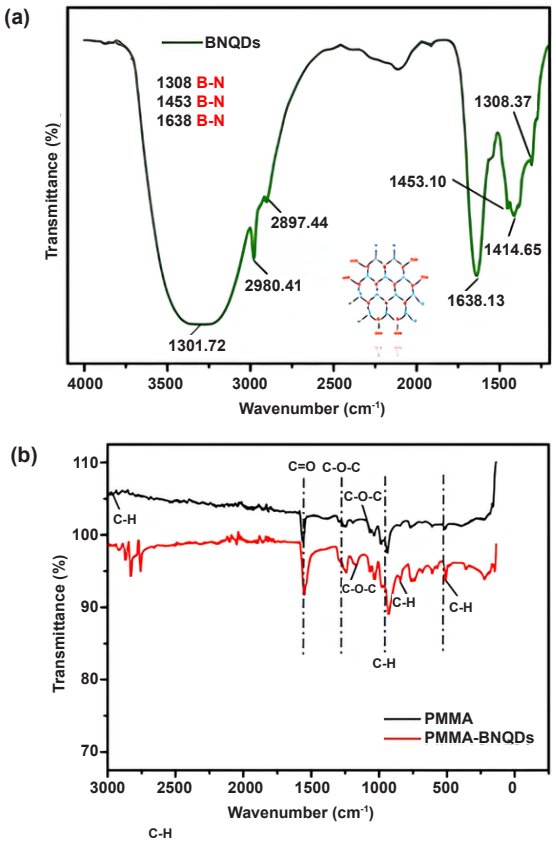

Figure 3. IR spectrum of BNQDs (a) and IR spectrum of PMMA and PMMA-BNQDs nanocomposite film (b)

BNQDs showed absorption bands at 1308, 1453, and 1638 cm^{-1}, respectively, due to the B-N stretching modes [8]. The band at 1414 cm^{-1} belongs to C-O bending [30]. The broad tensile band at 3300 cm^{-1} can be explained as the tensile band belonging to the N-H or O-H stretching. The appearance of the strains in the boron and nitrogen bonds and also functional groups such as -OH and $-NH_2$ in the IR spectra indicates that boron nitride was formed. FT-IR analysis is not sufficient to prove this. Therefore, the formation of quantum dots was supported by high-resolution TEM images. Figure 3b represents the IR spectrum of pure polymer and BNQDs polymer composite film. A sharp peak around 1730 cm^{-1} is consistent with the C=O stretching and stretching or deformation of C-O-C vibration peaks observed at 1249, 1164, and 1069 cm^{-1}. The peaks around 933 cm^{-1} and 844 cm^{-1} belong to the bending vibrations of C-H. The polymer chains have an absorption band around 750 cm^{-1} [31].

FTIR spectra of the PMMA-BNQDs nanocomposite film showed an absorption band at nearly 2970 cm^{-1} due to the C-H stretching vibration. Compared to the pure polymer, the peak intensities increased with the inclusion of boron nitride quantum dots into the structure at the stress intensity of 508 cm^{-1}, 928 cm^{-1}, and 1553 cm^{-1}, respectively. As a result of the modification of the polymer structure with the coating of boron nitride nanoparticles, the stretching band of the C-O-C shifted [32]. This shows that boron nitride nanoparticles are effectively incorporated into the PMMA polymer structure.

Figure 4 contains SEM images of PMMA and PMMA-BNQDs nanocomposite film at different magnifications. Figure 4 a,b shows the morphology of the PMMA polymer at magnifications of 25 and 75 kX, respectively. PMMA particles show a single type of morphology with a spherical shape and narrow size distribution [33]. Spherical particles are distributed with an average diameter of 0.15 μm. Figure 4 c,d contains the morphology of PMMA-BNQDs nanocomposite films at different magnifications. While some particles have smooth surfaces, some are coated with agglomerated BNQDs nanoparticles. The average size of these particles is 1.45μm, and it is clearly observed that they are larger than the pure PMMA polymer. This confirms a strong chemical electron affinity between BNQDs and PMMA, facilitating the formation of the core and shell [34].

Figure 5 shows the TEM image of the pure PMMA and PMMA-BNQDs nanocomposite film. In Figure 5a, PMMA shows a well-dispersed and forms an interconnected network-like structure [35]. In Figure 5b, the dark region refers to fluorescent particles and holes due to particle aggregation [36]. BNQDs have a significant agglomeration in some places in the polymer matrix. However, it is generally possible to say that the quantum dots are distributed homogeneously within the polymer. Figure 5c contains the HRTEM image of the obtained BNQDs. The average size

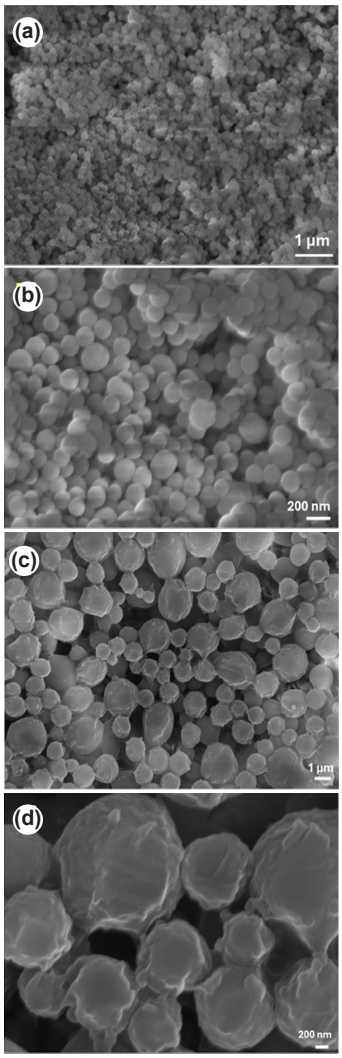

Figure 4. SEM images of the samples at different magnifications PMMA- 25 kX (a), PMMA-75 kX (b), PMMA-BNQDs-10 kX (c), PMMA-BNQDs-40 kX (d)

of quantum dots is 4.5 nm. High-resolution TEM images represent hexagonal boron nitride with high crystallinity and (002) the plane which confirms the production of BNQDs [37]. The surface morphology of PMMA-BNQDs nanocomposite film was identified by AFM with the scan size fixed to 1 μm × 1 μm (Figure 5d). The surface texture of polymer composites and the average size of the particles are also consistent with SEM and TEM images. The dispersed inorganic parts are homogeneously embedded in the polymer film. PMMA/BNQDs composite film comprises microspheres, as shown in the AFM histogram. The average size of BNQDs incorporated PMMA macro spheres is calculated as 1.6 μm. The size of these particles means that several interconnected quantum dots are embedded in the polymer [38].

Figure 6a shows the PL spectrum of PMMA-BNQDs nanocomposite film for 100 μM of different metal ions. In the spectrum, the emission peak for Ca^{2+}, Mg^{2+}, and Na^{+} was around 510 nm, while for Fe^{3+} and Zn^{2+}, this emission peak was observed around 538 and 540 nm, respectively.

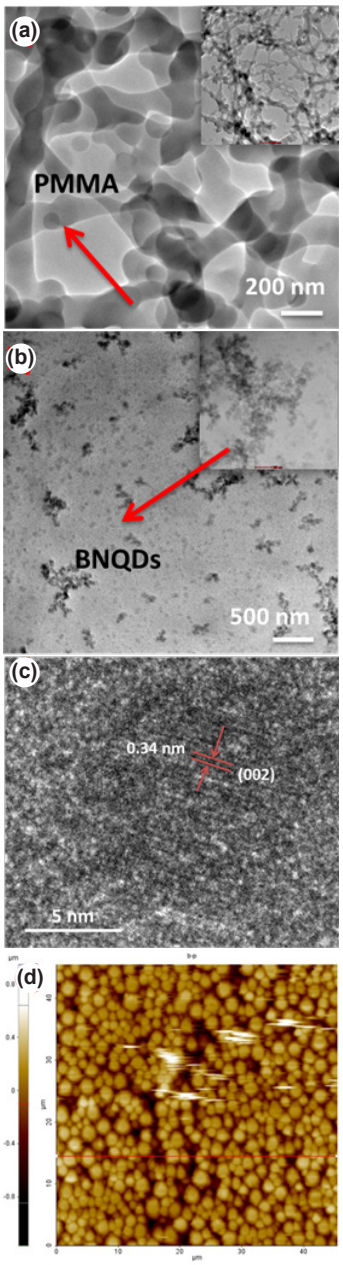

Figure 5. TEM image of pure PMMA sample (a), TEM image of PMMA-BNQDs nanocomposite film (b), HRTEM image of the BNQDs (c), and AFM image of the PMMA-BNQDs nanocomposite film (d)

This shift is seen more clearly in the normalized PL spectrum (Figure 6b). Here, the functional groups at the ends of BNQDs interact with metal ions and want to form stronger complexes with these metals [39]. Although there is no clear information about the fluorescence quenching mechanism for each metal, we assume that differences in the intermolecular interactions between different metals and composite films lead to different emission peaks in the fluorescence spectrum [40]. In their study, Wang et al. similarly observed that while the emission peak of BNQDs was observed at 461 nm, in the environment of Hg^{2+} ions, this emission peak shifted to 560 nm and created a fluorescence response against these ions. They interpreted the reason for this shift as the absorption of fluorescence from parts not connected to Hg^{2+} ions through induced electron transfer and internal filter effect [10]. There are many studies in the literature where BNQDs are used as sensors in liquid solution form in the detection of heavy metals, and it is clearly stated in these studies that the possible fluorescence response of the BNQDs against the Fe^{3+} ion is due to electron transfer [9, 11]. Boron nitride quantum dots interact with Fe^{3+} ions thanks to their rich amine groups and transfer the excited electrons to the half-filled orbitals of the Fe^{3+} ion. As a result of this excitation, the electron/hole part disappears, and fluorescence quenching occurs [41]. This quenching is apparently due to the affinity relationship of Fe^{3+} ions with the functional groups of BNQDs.

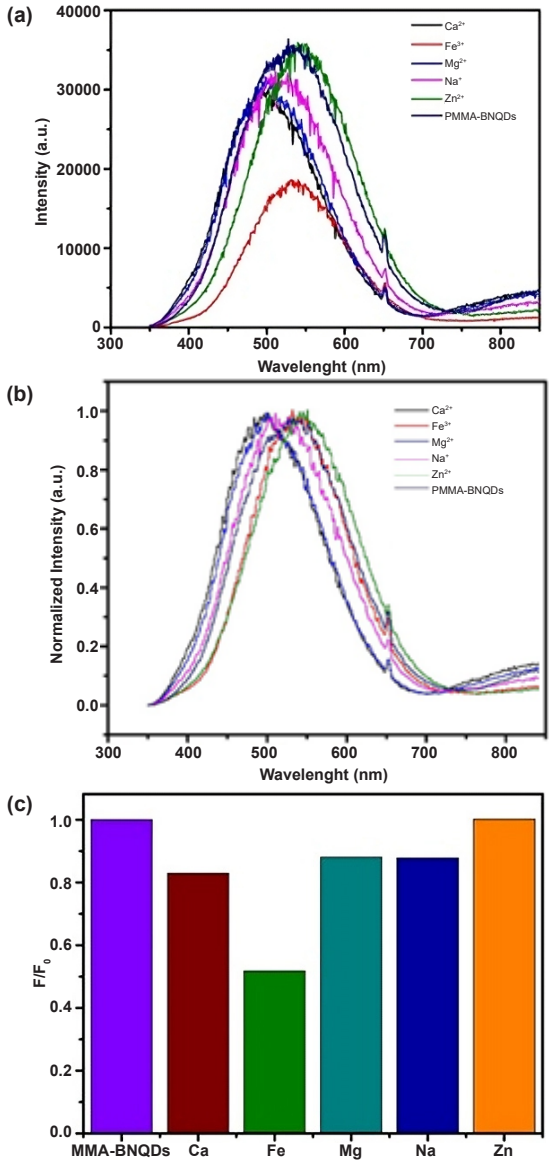

Figure 6. PL spectrum of PMMA-BNQDs nanocomposite film for 100 µM of different metal ions (a),normalized PL spectrum of PMMA-BNQDs nanocomposite film for 100 µM of different metal ions (b), selective fluorescence response of PMMA-BNQDs film towards 100 µM of different metal ions. F_0 and F represent the fluorescence intensity of PMMA/BNQDs film in the absence and presence of metal ions (c), respectively

The main reason for this affinity is that Fe^{3+} ions, which have paramagnetic properties, compensate for the electron deficiency on the surface of BNQDs. Due to the paramagnetic property of Fe^{3+}, it has high bonding interaction with electron-rich -OH or $-NH_2$ groups on the surface of BNQDs. These half-filled orbitals of the Fe^{3+} ion are very suitable for the transfer. The filling of these empty holes by these electrons results in the quenching of the fluorescence of the quantum dots [42,43]. In order to determine the selectivity of the obtained nanocomposite films, F/F_0 values were calculated for each metal using the PL spectra obtained in different metal ion solutions prepared at 100 µM concentration (Figure 6c). Zn^{2+} did not show any quenching effect. It can be seen clearly from Figure 6c that Ca^{2+}, Mg^{2+}, and Na^{+} show a slight quenching effect compared to Fe^{3+}. It is observed that the obtained PMMA-BNQDs nanocomposite sample has selectivity towards Fe^{3+} ion due to its high damping effect. For this reason, different concentrations of Fe^{3+} ions between 0-100 µM were prepared, and their absorbance and PL spectra were recorded.

Figure 7a shows the UV-Vis spectrum of PMMA-BNQDs nanocomposite film for different (0, 20, 45, 60, 80 and 100 µM) concentrations of Fe^{3+} ion. When nanocomposite films were immersed in Fe^{3+} solutions of different concentrations, it was observed that their absorbance values increased as the concentration of the metal ion increased. The linear increase in absorption intensity is related to the increase in complex formation, which leads to an increase in nanoparticle concentration. In general, this change in absorption intensity can be associated with an increase in particle size [44]. More importantly, it was observed that when the composites were immersed in Fe^{3+} solution, the peak of around 280 nm belonging to BNQDs disappeared, and the films showed a peak of around 260 nm. The disappearance of this peak compared to Figure 2a shows that the BNQDs surfaces are modified with Fe^{3+} ions and the films form complexes with Fe^{3+} ions [45]. Figure 7b represents the PL spectrum of PMMA-BNQDs nanocomposite film for different concentrations of Fe^{3+} ions. The fluorescence intensity of the nanocomposite films decreased with the increase in the concentration of Fe^{3+} ions. This can be associated with the fact that as the amount of Fe^{3+} ions in the medium increases, the empty orbitals of the Fe^{3+} ions are filled by electron transfer by quantum dots, thus increasing the damping demand and quenching of the films [42]. Figure 7c includes the relationship between F_0/F and Fe^{3+} ion concentration between 0-60 µM. While the calibration curve shows a linear trend between 0-60 µM, this trend does not exist between 0-100µM (Inset of Figure 7c). This shows that the sensitivity of the composite film above 60 µM is relatively low. For this reason, the LOD value and standard deviation were calculated for the 0-60 µM sensitivity level. The LOD value is the lowest value of a quantitatively specified signal, such as concentration and activity. In other words, it is known as the lowest

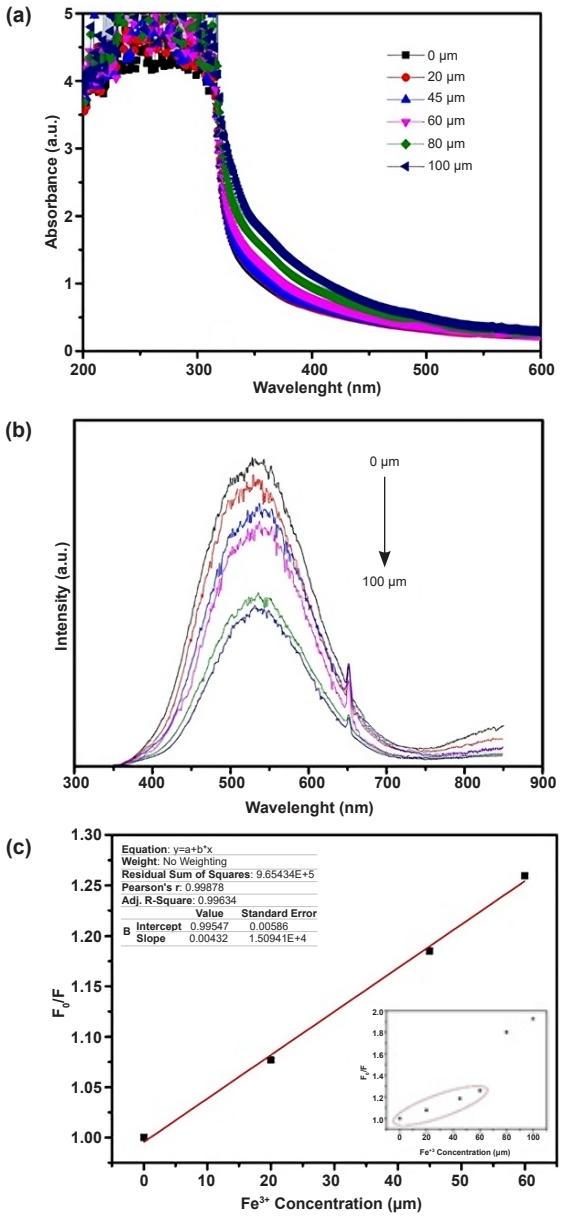

Figure 7. UV-Vis spectrum of PMMA-BNQDs nanocomposite film for different concentrations of Fe^{3+} ion (a), PL spectrum of PMMA-BNQDs nanocomposite film for different concentrations of Fe^{3+} ion (b), Calibration curve to present the relationship between fluorescence emission peak and Fe^{3+} concentration between 0-60 µM where F_0 and F are the fluorescence intensities in the absence and presence of Fe^{3+} ions (c), inset: calibration curve to present the relationship between fluorescence emission peak and Fe^{3+} concentration between 0-100 µM

amount of a matter that can be separated from the failure of that matter and identified within a given confidence interval [46]. According to the graph, the change in Fe^{3+} ion concentration between 0-60 µM showed a linear relationship, confirmed by the R^2 value of 0.99634. In addition, the standard deviation value of the linear curve is quite low (0.000150), which shows that the data points are distributed closer to the mean, the data set is not scattered, and small deviations are present [47].

This stable complex of Fe^{3+} with BNQDs confirms the static fluorescence quenching relationship.

On the other hand, the limit of detection (LOD) was calculated according to the following formula, where δ is the standard deviation [48]:

$$LOD = \frac{3\delta}{slope} \quad (1)$$

Using the data in Table 1, LOD was determined as 4.06 μM, lower than the Environmental Protection Agency (EPA) guidelines for drinking water of 5.37 μM [49].

Lv et al. obtained films from PVA and sulfur quantum dots that detected Fe^{3+} ions and found a limit of detection value of 0.69 μM. The stabilization of the polymer used here was quite effective. The fact that the sulfur quantum dots did not agglomerate in the polymer caused them to exhibit strong photoluminescence properties [28]. In another study, Gogoi et al. showed that the hydrogels they prepared using chitosan and carbon quantum dots had a detection limit of 0.0005 μM in detecting Fe^{3+} ions [50]. Compared with the results found here, the agglomeration and concentration of BNQDs in some areas within PMMA negatively affected the photoluminescence properties and LOD value. The sensor sensitivity ranges of composite materials can be improved by using different polymers. The results obtained were guiding in terms of directing the use of BNQDs in the detection of heavy metals in water by forming films with different polymers.

Table 1. Calibration data of PMMA-BNQDs nanocomposite film with Fe^{3+}

Parameter	Fe^{3+}
Regression equation	F_0/F=0.00432[μM]+0.99547
Slope	0.00432
Intercept	0.99547
R^2	0.99634
Correlation coefficient (r)	0.99878
Linear range	0-60 μM
SD of intercept	0.00586
SD of slope	0.000150
LOD	4.06 μM

4. Conclusions

Herein, PMMA-BNQDs nanocomposite film was successfully synthesized as a fluorescence test surface to identify metal ions in water selectively. Various characterization techniques have demonstrated the morphological structure of nanocomposite films and the chemical groups they contain. While FT-IR and HR-TEM analysis proved the existence of BNQDs, the structural analysis of the films was supported by FT-IR, SEM, TEM, and AFM analyses. It was determined that the obtained films showed selective fluorescence quenching properties against Fe^{3+}. The fluorescence intensities of the films showed a linear relationship between 0-60 μM and were calculated to have a LOD value of 4.06 μM. This reveals that this fluorescence sensing platform can selectively and sensitively detect Fe^{3+} ions in drinking water between 0-60 μM. Fluorescence quenching is apparently due to the affinity relationship of Fe^{3+} ions with the functional groups of BNQDs. These groups attached to the surface of BNQDs are electron-rich groups and show high interaction due to the paramagnetic properties of Fe^{3+} ions. This study has guided the use of boron nitride quantum dot-based polymer nanocomposite films as fluorescence sensing platforms, and it also offers an innovative and practical application approach for the use of polymer-based composite structures in the detection of metal ions.

5. Author Contribution Statement

Duygu Kuru: Conceptualization, methodology, data curation, writing-original draft preparation, visualization, investigation, validation, writing-review, and editing.

References

[1] Dawoud, H. D., Saleem, H., Alnuaimi, N. A., & Zaidi, S. J. (2021). Characterization and treatment technologies applied for produced water in Qatar. *Water*, *13*(24), 3573. https://doi.org/10.3390/w13243573

[2] Soliman, M.N., Guen, F.Z., Ahmed, S.A., Saleem, H., & Zaidi, S.J. (2002) Environmental impact assessment of desalination plants in the gulf region. In V. Naddeo, K. H. Choo, M. Ksibi (Eds.), *Water-energy-nexus in the ecological transition*. Advances in science, technology & innovation (pp. 173-177). Springer, Cham.. https://doi.org/10.1007/978-3-031-00808-5_41

[3] Saleem, H., Zaidi, S. J., Ismail, A. F., Goh, P. S., & Vinu, A. (2022). Recent advances in the application of carbon nitrides for advanced water treatment and desalination technology. *Desalination*, *542*, 116061. https://doi.org/10.1016/j.desal.2022.116061

[4] Saud, A., Saleem, H., Munira, N., Shahab, A. A., Siddiqui, H. R., & Zaidi, S. J. (2023). Sustainable preparation of graphene quantum dots for metal ion sensing application. *Nanomaterials*, *13*(1), 148. https://doi.org/10.3390/nano13010148

[5] Li, Q., Zhou, W., Yu, L., Lian, S., & Xie, Q. (2021). Perovskite quantum dots as a fluorescent probe for metal ion detection in aqueous solution via phase transfer. *Materials Letters, 282*, 128654. https://doi.org/10.1016/j.matlet.2020.128654

[6] Bian, S., Shen, C., Hua, H., Zhou, L., Zhu, H., Xi, F., … & Dong, X. (2016). One-pot synthesis of sulfur-doped graphene quantum dots as a novel fluorescent probe for highly selective and sensitive detection of lead(II). *RSC Advances*, *6*(74), 69977-69983. https://doi.org/10.1039/C6RA10836A

[7] Huo, B., Liu, B., Chen, T., Cui, L., Xu, G., Liu, M., & Liu, J. (2017). One-step synthesis of fluorescent boron

nitride quantum dots via a hydrothermal strategy using melamine as nitrogen source for the detection of ferric ions. *Langmuir*, *33*(40), 10673-10678. https://doi.org/10.1021/acs.langmuir.7b01699

[8] Liu, B., Yan, S., Song, Z., Liu, M., Ji, X., Yang, W., & Liu, J. (2016). One-step synthesis of boron nitride quantum dots: Simple chemistry meets delicate nanotechnology. *Chemistry A European Journal*, *22*(52), 18899-18907. https://doi.org/10.1002/chem.201603935

[9] Peng, D., Zhang, L., Li, F., Cui, W., Liang, R., & Qui, J. (2018). Facile and green approach to the synthesis of boron nitride quantum dots for 2,4,6-trinitrophenol sensing. *ACS Applied Materials Interfaces*, *10*(8), 7315-7323. https://doi.org/10.1021/acsami.7b15250

[10] Wang, L., Zhang, Q., Su, P., Yu, L., Bu, Y., Yuan, C., & Wang, S. (2022). Excitation-dependent ratiometric fluorescence response to mercury ion based on single hexagonal boron nitride quantum dots. *Analytica Chimica Acta*, *1236*, 340585. https://doi.org/10.1016/j.aca.2022.340585

[11] Han, Y., Niu, Y., Liu, M., Niu, F., & Xu, Y. (2019). A rational strategy to develop a boron nitride quantum dot-based molecular logic gate and fluorescent assay of alkaline phosphatase activity. *Journal of Materials Chemistry B*, *7*(6), 897-902. https://doi.org/10.1039/C8TB02948B

[12] Yu, X., Yang, L., Zhao, T., Zhang, R., Yang, L., Jiang, C., … & Zhang, Z. (2017). Multicolorful ratiometric-fluorescent test paper for determination of fluoride ions in environmental water. *RSC Advances*, *7*(5), 53379-53384. https://doi.org/10.1021/am506558d

[13] Cheng, Z., Liu, X., Zhao, B., Liu, X., Yang, X., Zhang, X., & Feng, X. (2024). A portable europium complex-loaded fluorescent test paper combined with smartphone analysis for the on-site and visual detection of mancozeb in food samples. *Food Chemistry*, *458*, 140311. https://doi.org/10.1016/j.foodchem.2024.140311

[14] Huang, T., Xu, Y., Meng, M., & Li, C. (2022). PVDF-based molecularly imprinted ratiometric fluorescent test paper with improved visualization effect for catechol monitoring. *Microchemical Journal*, *178*, 107369. https://doi.org/10.1016/j.microc.2022.107369

[15] Wang, C., Sun, Y., Jin, J., Xiong, Z., Li, D., Yao, J., & Liu, Y. (2018). Highly selective, rapid-functioning and sensitive fluorescent test paper based on graphene quantum dots for on-line detection of metal ions. *Analytical Methods*, *10*(10), 1163-1171. https://doi.org/10.1039/C7AY02995K

[16] Dalal, C., Garg, A. K., Mathur, M., & Sonkar, S. K. (2022). Fluorescent polymer carbon dots for the sensitive-selective sensing of Fe3+ metal ions and cellular imaging. *ACS Applied Nano Materials*, *5*(9), 12699-12710.https://doi.org/10.1021/acsanm.2c02544

[17] Shirani, M. P., Rezaei, B., Ensafi, A. A., & Ramezani, M. (2021). Development of an eco-friendly fluorescence nanosensor based on molecularly imprinted polymer on silica-carbon quantum dot for the rapid indoxacarb detection. *Food Chemistry*, *339*, 127920.https://doi.org/10.1016/j.foodchem.2020.127920

[18] Ma, Y., Cao, X., Feng, X., Ma, Y., & Zou, H. (2007). Fabrication of super-hydrophobic film from PMMA with intrinsic water contact angle below 90. *Polymer*, *48*(26), 7455-7460. https://doi.org/10.1016/j.polymer.2007.10.038

[19] Cui, Z., Martinez, A. P., & Adamson, D. H. (2015). PMMA functionalized boron nitride sheets as nanofillers. *Nanoscale*, *7*(22), 10193-10197.https://doi.org/10.1039/C5NR00936G

[20] Liu, F., Li, Q., Li, Z., Liu, Y., Dong, L., Xiong, C., & Wang, Q. (2017). Poly(methyl methacrylate)/boron nitride nanocomposites with enhanced energy density as high temperature dielectrics. *Composites Science and Technology*, *142*, 139-144.https://doi.org/10.1016/j.compscitech.2017.02.006

[21] Wang, Y., Zhu, Y., Huang, J., Cai, J., Zhu, J., Yang, X., & Li, C. (2017). Perovskite quantum dots encapsulated in electrospun fiber membranes as multifunctional supersensitive sensors for biomolecules, metal ions and pH. *Nanoscale Horizons*, *2*(4), 225-232. https://doi.org/10.1039/C7NH00057J

[22] Wang, Q., Sun, G., Wei, S., Hao, W., & Yang, W. (2021). HPAMAM/PMMA composite electrospun film for cobalt ion detection in water environments. *Materials Letters*, *299*, 130115. https://doi.org/10.1016/j.matlet.2021.130115

[23] Tajik, S., Beitollahi, H., Nejad, F. G., Dourandish, Z., Khalilzadeh, M. A., Jang, H. W., … & Shokouhimehr, M. (2021). Recent developments in polymer nanocomposite-based electrochemical sensors for detecting environmental pollutants. *Industrial & Engineering Chemistry Research*, *60*(3), 1112-1136. https://doi.org/10.1021/acs.iecr.0c04952

[24] Emir, P., & Kuru, D. (2024). Boron nitride quantum dots/polyvinyl butyral nanocomposite films for the enhanced photoluminescence and UV shielding properties. *Journal of Applied Polymer Science*, *141*(13), e55171. https://doi.org/10.1002/app.55171

[25] Yang, Y., Zhang, C., Huang, D., Zeng, G., Huang, J., Lai, C., … & Xiong, W. (2019). Boron nitride quantum dots decorated ultrathin porous g-C3N4: Intensified exciton dissociation and charge transfer for promoting visible-light-driven molecular oxygen activation. *Applied Catalysis B: Environmental*, *245*, 87-99. https://doi.org/10.1016/j.apcatb.2018.12.049

[26] Liu, M., Xu, Y., Wang, Y., Chen, X., Ji, X., Niu, F., Song, Z., & Liu, J. (2017). Boron nitride quantum dots with solvent-regulated blue/green photoluminescence and electrochemiluminescent behavior for versatile applications. *Advanced Optical Materials*, *5*(3), 1600661. https://doi.org/10.1002/adom.201600661

[27] Abdelsalam, H., & Zhang, Q. F. (2022). Properties and applications of quantum dots derived from two-dimensional materials. *Advances in Physics: X*, *7*(1), 2048966. https://doi.org/10.1080/23746149.2022.2048966

[28] Lv, G., Dai, X., Lu, G., Ye, L., Wang, G., & Zhou, L. (2023). Facile fabrication of portable electrospun poly(vinyl alcohol)/sulfur quantum dots film sensor for sensitive and selective detection of Fe3+. *Optical Materials*, *135*, 113227.https://doi.org/10.1016/j.optmat.2022.113227

[29] Sekar, A., Yadav, R., & Basavaraj, N. (2021). Fluorescence quenching mechanism and the application of green carbon nanodots in the detection of heavy metal ions: A review. *New Journal of Chemistry*, *45*(5), 2326-2360. https://doi.org/10.1039/D0NJ04878J

[30] Mohan Babu, M., Syam Prasad, P., Venkateswara Rao, P., Hima Bindu, S., Prasad, A., Veeraiah, N., & Özcan, M. (2020). Influence of ZrO2 addition on structural and biological activity of phosphate glasses for bone regeneration. *Materials*, *13*(18), 4058.https://doi.org/10.3390/ma13184058

[31] Mthethwa, T. P., Moloto, M. J., Vries, A. D., & Matabola, K. P. (2011). Properties of electrospun CdS and CdSe filled poly(methyl methacrylate) (PMMA) nanofibres. *Materials Research Bulletin*, *46*(4), 569-575. https://doi.org/10.1016/j.materresbull.2010.12.022

[32] Alqahtani, M. (2020). Effect of hexagonal boron nitride nanopowder reinforcement and mixing methods on physical and mechanical properties of self-cured PMMA for dental applications. *Materials*, *13*(10), 2323. https://doi.org/10.3390/ma13102323

[33] Khan, F. A., Akhtar, S., Almohazey, D., Alomari, M., Almofty, S. A., Badr, I., & Elaissari, A. (2019). Targeted delivery of poly (methyl methacrylate) particles in colon cancer cells selectively attenuates cancer cell proliferation. Artificial Cells, *Nanomedicine, and Biotechnology*, *47*(1), 1533-1542. https://doi.org/10.1080/21691401.2019.1577886

[34] Meng, X., Cui, H., Dong, J., Zheng, J., Zhu, Y., Wang, Z., … & Zhu, Z. (2013). Synthesis and electrocatalytic performance of nitrogen-doped macroporous carbons. *Journal of Materials Chemistry A*, *1*, 9469-9476. https://doi.org/10.1039/C3TA10306D

[35] Pawar S., Rzeczkowski P. P., Pötschke P., Krause B., & Bose S. (2018). Does the processing method resulting in different states of an interconnected network of multiwalled carbon nanotubes in polymeric blend nanocomposites affect EMI shielding properties? *ACS Omega*, *3*(5), 5771-5782. https://doi.org/10.1021/acsomega.8b00575

[36] Yoon, C., Yang, K. P., Kim, J., & Shin, K. (2020). Fabrication of highly transparent and luminescent quantum dot/polymer nanocomposite for light emitting diode using amphiphilic polymer-modified quantum dots. *Chemical Engineering Journal*, *382*, 122792. https://doi.org/10.1016/j.cej.2019.122792

[37] Lin, L., Xu, Y., Zhang, S., Ross, I. M., Ong, A. C. M., & Allwood, D. A. (2014). Fabrication and luminescence of monolayered boron nitride quantum dots. *Small*, *10*(1), 60-65. https://doi.org/10.1002/smll.201301001

[38] Poderys, V., Matulionyte, M., Selskis, A., & Rotomskis, R. (2011). Interaction of water-soluble cdte quantum dots with bovine serum albumin. *Nanoscale Research Letters*, *6*(9). https://doi.org/10.1007/s11671-010-9740-9

[39] Wu, F., Tong, H., Wang, K., Wang, Z., Li, Z., Zhu, X., … & Wong, W. K. (2016). Synthesis, structural characterization and photophysical studies of luminescent Cu(I) heteroleptic complexes based on dipyridylamine. *Journal of Photochemistry and Photobiology A: Chemistry*, *318*, 97-103. https://doi.org/10.1016/j.jphotochem.2015.12.003

[40] Upadhyay, P. K., Marpu, S. B., Benton, E. N., Williams, C. L., Telang, A., & Omary, M. A. (2018). A phosphorescent trinuclear gold(I) pyrazolate chemosensor for silver ion detection and remediation in aqueous media. *Analytical Chemistry*, *90*(8), 4999-5006. https://doi.org/10.1021/acs.analchem.7b04334

[41] Yao, Q., Feng, Y., Rong, M., He, S., & Chen, X. (2017). Determination of nickel(II) via quenching of the fluorescence of boron nitride quantum dots. *Mikrochima Acta*, *184*, 4217-4223. https://doi.org/10.1007/s00604-017-2496-5

[42] Chen, Y., Wu, Y., Bo, W., Wang, B., & Li, C. (2016). Facile synthesis of nitrogen and sulfur co-doped carbon dots and application for Fe(III) ions detection and cell imaging. *Sensors and Actuators B: Chemical*, 223, 689-696. https://doi.org/10.1016/j.snb.2015.09.081

[43] Ahmadian-Fard-Fini, S., Ghanbari, D., Amiri, O., & Salavati-Niasari, M. (2020). Electro-spinning of cellulose acetate nanofibers/fe/carbon dot as photoluminescence sensor for mercury (ii) and lead (ii) ions. *Carbohydrate Polymers*, *229*, 115428-115428. https://doi.org/10.1016/j.carbpol.2019.115428

[44] Islam, N. U., Amin, R., Shahid, M., Amin, M., Zaib, S., & Iqbal, J. (2017). A multi-target therapeutic potential of Prunus domestica gum stabilized nanoparticles exhibited prospective anticancer, antibacterial, urease-inhibition, anti-inflammatory and analgesic properties. *BMC Complementary and Alternative Medicine*, *17*(1), 276. https://doi.org/10.1186/s12906-017-1791-3

[45] Zhao, L., Wang, Y., Zhao, X., Deng, Y., & Xia, Y. (2019). Facile synthesis of nitrogen-doped carbon quantum dots with chitosan for fluorescent detection of Fe3+. *Polymers*, *11*(11), 1731. https://doi.org/10.3390/polym11111731

[46] Rajaković, L. V., Marković, D. D., Rajaković-Ognjanović, V. N., & Antanasijević, D. Z. (2012). The approaches for estimation of limit of detection for ICP-MS trace analysis of arsenic. *Talanta*, *102*, 79-87. https://doi.org/10.1016/j.talanta.2012.08.016

[47] Armbruster, D. A., & Pry, T. (2008). Limit of blank, limit of detection and limit of quantitation. *The Clinical Biochemist Reviews*, *29*(Suppl 1), 49-52. Retrieved from https://pubmed.ncbi.nlm.nih.gov/18852857/

[48] Khairy, G. M., Amin, A. S., Moalla, S. M. N., Medhat, A., & Hassan, N. (2022). Fluorescence determination of Fe(III) in drinking water using a new fluorescence chemosensor. *RSC Advances*, *12*(42), 27679-27686. https://doi.org/10.1039/d2ra05144c

[49] Liu, X., Li, N., Xu, M., Wang, J., Jiang, C., Song, G., & Wang, Y. (2018). Specific colorimetric detection of Fe3+ ions in aqueous solution by squaraine-based chemosensor. *RSC Advances*, *8*(61), 34860-34866. https://doi.org/10.1039/C8RA07345G

[50] Gogoi, N., Barooah, M., Majumdar, G., & Chowdhury, D. (2015). Carbon dots rooted agarose hydrogel hybrid platform for optical detection and separation of heavy metal ions. *ACS Applied Materials & Interfaces*, *7*(5), 3058-3067.https://doi.org/10.1021/am506558d